ELSEVIER

Physica D 150 (2001) 1–13

PHYSICA D

www.elsevier.com/locate/physd

Pseudo-riddling in chaotic systems

Ying-Cheng Lai

Departments of Mathematics, Electrical Engineering, and Physics, Center for Systems Science and Engineering Research, Arizona State University, Tempe, AZ 85287, USA

Received 24 May 2000; accepted 19 December 2000
Communicated by Y. Kuramoto

Abstract

Previous investigations of riddling have focused in the case where the dynamical invariant set in the symmetric invariant subspace of the system is a chaotic attractor. A situation expected to arise commonly in dynamical systems, however, is that the dynamics in the invariant subspace is in a periodic window. In such a case, there are both a stable periodic attractor and a coexisting non-attracting chaotic saddle in the invariant subspace. We show that riddling can still occur in a generalized sense. In particular, we argue that the basin of the periodic attractor in the invariant subspace contains both an open set and a set of measure zero with riddled holes that belong to the basin of another attractor. We call such basin *pseudo-riddled* and we argue that pseudo-riddling can be more pervasive than riddling of chaotic attractors because it can occur regardless of whether the chaotic saddle in the invariant subspace is transversely stable or unstable. We construct an analyzable model, derive a scaling law for pseudo-riddling, and provide numerical support. We also show that the chaotic saddle in the invariant subspace can undergo an enlargement into the full phase space when it becomes transversely unstable. © 2001 Published by Elsevier Science B.V.

PACS: 05.45.Jn; 05.45.Ac

Keywords: Pseudo-riddling; Dynamical invariant set; Chaotic; Saddle

1. Introduction

Riddling is a recently studied phenomenon that occurs in chaotic systems with a symmetric invariant subspace [1–8]. The phenomenon has attracted much attention because it is fairly common for dynamical systems to have a simple symmetry that often leads to the existence of an invariant subspace. For instance, in spatially extended chaotic systems such as those described by coupled maps or coupled differential equations, there is a natural invariant subspace: the synchronization manifold on which all individual oscillators evolve chaotically and synchronously in time [9–11].

The dynamical conditions for riddling to occur are first described in [2] where it is shown that for systems with an invariant subspace $\mathcal{M}$: (i) if there is a chaotic attractor in $\mathcal{M}$, and (ii) if a typical trajectory in the chaotic attractor is stable with respect to perturbations transverse to $\mathcal{M}$, then the basin of the chaotic attractor in $\mathcal{M}$ can be riddled with holes that belong to the basin of another attractor off $\mathcal{M}$, provided that such an attractor exists. That is, for every initial condition that asymptotes to the chaotic attractor in $\mathcal{M}$, there are initial conditions arbitrarily nearby

E-mail address: yclai@chaos1.la.asu.edu (Y.-C. Lai).

0167-2789/01/$ – see front matter
PII: S0167-2789(00)00226-8

that asymptote to the attractor off $\mathcal{M}$. The mechanism for riddling to occur and the basin structure associated with riddling are investigated [6]. Riddled basins are also studied in experiments conducted using coupled electrical oscillators [4]. More recently, it is discovered and analyzed that small random noise can induce riddling in much larger parameter regimes, even in those in which riddling would previously be thought not to occur [7].

Previous research has been based on the assumption that conditions (i) and (ii) are necessary for riddling to occur. In this work, we argue that one of the conditions — condition (i) — the existence of a chaotic attractor in the invariant subspace $\mathcal{M}$, is only sufficient but not necessary. It is necessary, however, that a chaotic invariant set does exist in $\mathcal{M}$. It is thus sufficient to have a non-attracting chaotic saddle in $\mathcal{M}$ to have riddling (in a generalized sense). These findings have dynamical consequences to practical problems. While chaotic attractors are common in physical systems, it can easily disappear as a system parameter undergoes arbitrarily small changes [12]. For instance, the dynamics in the invariant subspace may be that of one of the infinite number of periodic windows near a parameter value at which the chaotic attractor is observed. Since, periodic windows occupy intervals of parameter values which are apparently dense [13] in the parameter space, we expect the situation to be common in nonlinear systems. At a given periodic window, one finds the coexistence of a non-attracting chaotic saddle and an attracting periodic orbit [14]. A question is then, how does riddling manifest itself when the dynamics in the invariant subspace is in a periodic window whose invariant sets are both a non-attracting chaotic saddle (necessary condition (i) for riddling) and an attracting periodic orbit? The purpose of this paper is to address this question in view of the stated necessary conditions for riddling. We find that riddling in fact occurs in the transverse vicinity of the chaotic saddle. Moreover, the basin of attraction in the transverse vicinity of the stable periodic orbit also consists of open volumes (open areas in two dimensions). Globally, the basin of attraction of the stable periodic orbit is therefore of a mixed type: open volumes and riddled-like structures. We call this type of basin *pseudo-riddled basins*. A surprising finding is that pseudo-riddling occurs in a wide parameter region for both transversely stable or transversely unstable chaotic saddles, a phenomenon that is in contrast to riddling with chaotic attractors, where riddling occurs only when the attractor is transversely stable with some of the embedded unstable periodic orbits being transversely unstable. To quantify pseudo-riddling, we investigate scaling laws for physically observable quantities such as the probability for a random initial condition to asymptote to different attractors. An implication of our results is that a riddling-like phenomenon can arise regardless of the nature of the attracting set in the invariant subspace, in so far as there is chaos (attracting or non-attracting) in the system. A brief account of these results has been published recently [15].

Another issue we address in this paper concerns the parametric evolution of a chaotic saddle as it becomes transversely unstable. In the case of a chaotic attractor, it has been known that the loss of its transverse stability can lead to dynamical phenomenon such as on–off intermittency [16–23]. Here, we investigate how the chaotic saddle, which is restricted to the invariant subspace when it is transversely stable, evolves after it becomes transversely unstable. We find that the chaotic saddle can extend into the entire phase space after the bifurcation, a phenomenon that is called *metamorphosis* of a chaotic saddle [24].

The paper is organized as follows. In Section 2, we give a qualitative argument for the phenomenon of pseudo-riddling. In Section 3, we present numerical evidence and scaling results for pseudo-riddling. A simple analytic model for which pseudo-riddling and the associated scaling behavior can be understood fairly completely is presented in Section 4. In Section 5, we study the evolution of the chaotic saddle after it loses its transverse stability. A brief discussion is presented in Section 6.

2. Pseudo-riddled basins

We present a qualitative argument for the condition under which pseudo-riddling can be observed. Let $\mathcal{M}$ be the invariant subspace in which there is a non-attracting chaotic saddle $\mathcal{S}$ and an attracting periodic orbit $\mathcal{O}$, and let **A** be

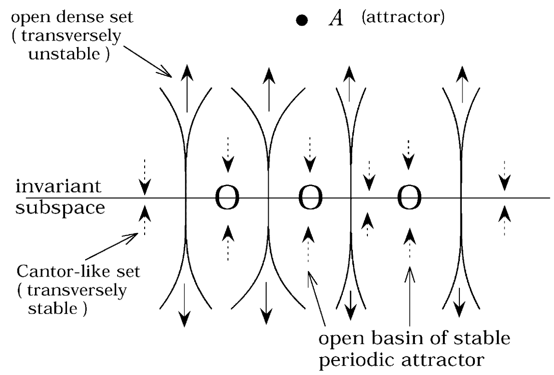

Fig. 1. A schematic illustration of the dynamical setting for pseudo-riddling: a chaotic saddle and an attracting periodic orbit $\mathcal{O}$ in the invariant subspace, and an attractor **A** off the invariant subspace. Points in the invariant subspace corresponding to the open dense set and the Cantor-like set belong to the chaotic saddle. The periodic attractor $\mathcal{O}$ is transversely stable, while the chaotic saddle can be either transversely stable or transversely unstable for pseudo-riddling to occur.

an attractor off $\mathcal{M}$, as shown schematically in Fig. 1. Assume that the periodic attractor $\mathcal{O}$ is transversely stable so that there is a boundary between the basins of attraction of $\mathcal{O}$ and **A**. Since $\mathcal{O}$ is stable both in $\mathcal{M}$ and in the transverse direction, the basin of attraction in the transverse vicinity of $\mathcal{O}$ is an open set containing $\mathcal{O}$ with finite volume. Now consider the situation where all unstable periodic orbits embedded in the chaotic saddle $\mathcal{S}$ are transversely stable. In this case, almost all initial conditions in the vicinity of $\mathcal{M}$ asymptote to the periodic attractor in $\mathcal{M}$. There is no riddling in this case. As a system parameter p changes through a critical value p_c, one of the unstable periodic orbits in $\mathcal{S}$ becomes transversely unstable and, as a consequence, a set of infinite number of tongues opens at the location of the periodic orbit and all its pre-images [6]. The situation so described is the riddling bifurcation that marks the onset of pseudo-riddling for $p > p_c$.

Can pseudo-riddling be observed in numerical experiments when p passes through the riddling bifurcation point? The answer to this question lies in the interplay between two important time scales: the lifetime of the chaotic saddle τ_O and another time associated with the riddling bifurcation. It was shown in [6] that for $p > p_c$, trajectories in the vicinity of $\mathcal{M}$ can typically spend an extremely long time near $\mathcal{M}$ before asymptoting to attractor **A** — a superpersistent chaotic transient. The lifetime of the transient scales with $\Delta p \equiv |p - p_c|$ as

$$\tau_A \sim \exp[K(\Delta p)^{-\gamma}],$$

where $\gamma > 0$ and $K > 0$. There is a practically important difference in the dynamics for $p > p_c$ between the case treated in [6], where the invariant set in $\mathcal{M}$ is a chaotic attractor, and our case here. In our case, supertransient still occurs but the lifetime τ_O associated with the chaotic saddle is typically much shorter than the supertransient lifetime: $\tau_O \ll \tau_A$. That is, a trajectory in the basin of the periodic attractor $\mathcal{O}$ approaches this attractor in a time that is typically shorter than the time τ_A it takes a trajectory in the basin of the attractor **A** to approach this attractor. As a practical consequence, no riddling can be observed, say in numerical experiments, immediately after the riddling bifurcation, until $\tau_O \sim \tau_A$. As Δp increases, τ_A decreases and becomes smaller than or equivalent to τ_O. In this case, it is easier to observe pseudo-riddling.

To observe pseudo-riddling in numerical or laboratory experiments, a large number of unstable periodic orbits embedded in the chaotic saddle $\mathcal{S}$ must be transversely unstable so that there is a physically realizable probability that a trajectory with a random initial condition can asymptote to the attractor **A**. We should restate that pseudo-riddling can occur *regardless of whether $\mathcal{S}$ itself is transversely stable or unstable*. Mathematically, the basin of attraction of **A** consists of an open dense set of tongues off the invariant subspace $\mathcal{M}$ but these tongues are restricted to the set $\mathcal{S}$. Note that this type of riddling is different from riddling of a chaotic attractor in $\mathcal{M}$, in which case riddling disappears when the attractor becomes transversely unstable [1–8]. In this sense, we expect pseudo-riddling to be more pervasive.

3. Numerical example

We consider the following general class of dynamical systems:

$$\mathbf{x}_{n+1} = \mathbf{f}(\mathbf{x}_n, r) + \text{higher order terms of } \mathbf{y}_n, \qquad \mathbf{y}_{n+1} = g(\mathbf{x}_n, a)\mathbf{y}_n + \text{higher order terms of } \mathbf{y}_n, \tag{1}$$

where $\mathbf{x} \in R^{N_\mathrm{S}}$ ($N_\mathrm{S} \geq 1$), $\mathbf{y} \in R^{N_\mathrm{T}}$ ($N_\mathrm{T} \geq 1$), $\mathbf{f}(\mathbf{x}_n, r)$ is a map possessing an infinite number of periodic windows, $g(\mathbf{x}_n, a)$ is a scalar function, r and a are parameters. The invariant subspace is defined by $\mathbf{y} = 0$ because for initial condition $\mathbf{y}_0 = \mathbf{0}$, trajectories have $\mathbf{y}_n = \mathbf{0}$ for all times. We choose the parameter r in the map $\mathbf{f}(\mathbf{x}_n, r)$ so that it is in a periodic window of period m. Let $\{\mathbf{x}_n^\mathrm{S}\}_{n=1}^{\infty}$ be a dense trajectory in the chaotic saddle and let $\{\mathbf{x}_1^\mathrm{O}, \mathbf{x}_2^\mathrm{O}, \ldots, \mathbf{x}_m^\mathrm{O}\}$ be the attracting periodic orbit in the window. The largest transverse Lyapunov exponents of the chaotic saddle and the periodic attractor are given by

$$\Lambda_\mathrm{T}^\mathrm{S} = \lim_{M\to\infty} \frac{1}{M} \sum_{n=1}^{M} \ln |g(\mathbf{x}_n^\mathrm{S}, a)\mathbf{I} \cdot \mathbf{u}|, \qquad \Lambda_\mathrm{T}^\mathrm{O} = \frac{1}{p} \sum_{i=1}^{m} \ln |g(\mathbf{x}_i^\mathrm{O}, a)\mathbf{I} \cdot \mathbf{u}|, \tag{2}$$

where $\mathbf{I}$ is the identity matrix and $\mathbf{u}$ a random unit vector in the transverse subspace. To be concrete, we study the following two-dimensional map:

$$x_{n+1} = rx_n(1 - x_n) + by_n^2, \qquad y_{n+1} = ax_n y_n + cy_n^3, \tag{3}$$

where $f(x) = rx(1 - x)$ is the logistic map, a, b, and c are parameters. We choose $r = 3.84$ so that the logistic map is in the period-3 window in which there is an attracting periodic orbit of period-3 coexisting with a chaotic saddle, as shown in Fig. 2(a), where the chaotic saddle is represented by a trajectory of 50 000 points obtained by using the PIM-triple method [25]. We are interested in the case where $\Lambda_\mathrm{T}^\mathrm{O}$ remains negative. There are thus two attractors in the system: the period-3 attractor in the invariant subspace $y = 0$ and the attractor at $y = +\infty$. Fig. 2(b) shows $\Lambda_\mathrm{T}^\mathrm{S}$ and $\Lambda_\mathrm{T}^\mathrm{O}$ versus a in the range $1.5 \leq a \leq 2.0$ for $b = 0.1$ and $c = 1.0$, where, as a is increased from 1.5, $\Lambda_\mathrm{T}^\mathrm{S}$ passes through zero from the negative side at $a_\mathrm{c} \approx 1.75$, while $\Lambda_\mathrm{T}^\mathrm{O}$ remains negative in this range of a. Figs. 3(a) and (b) show the basin of the period-3 attractor for $a = 1.7$ ($\Lambda_\mathrm{T}^\mathrm{S} \approx -0.034$) and $a = 1.8$ ($\Lambda_\mathrm{T}^\mathrm{S} \approx 0.023$), respectively. For both cases, the basin of the period-3 attractor appears pseudo-riddled, as can be verified through successive blowups of the basin near $y = 0$, *regardless of whether the chaotic saddle in* $y = 0$ *is transversely stable or transversely unstable*. The basin of the attraction at infinity is an open dense set of tongues in the transverse neighborhood of $\mathcal{S}$ in both figures.

To quantify pseudo-riddling, we focus on the scaling behaviors of some physical observables. In particular, we consider the probability for an initial condition chosen randomly from a line at $y = \epsilon$ near the invariant subspace $y = 0$ to asymptote to the attractor at infinity. Denote this probability by $F^+(\epsilon)$. Figs. 4(a) and (b) show $F^+(\epsilon)$ versus ϵ on a logarithmic scale for $a = 1.7$ and 1.8, respectively. Apparently, we have, for both cases, the following algebraic scaling law:

$$F^+(\epsilon) \sim \epsilon^\gamma, \tag{4}$$

where the scaling exponent is $\gamma \approx 1.73$ and 0.92 for Figs. 4(a) and (b), respectively. Note the scaling exponent in Fig. 4(a) is significantly larger than that for the case where there is a chaotic attractor in the invariant subspace

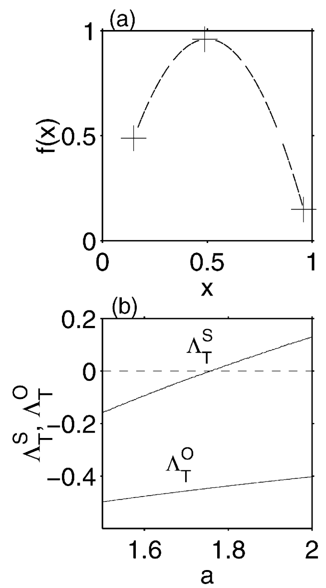

Fig. 2. (a) The chaotic saddle and the periodic attractor in the period-3 window of the logistic map. (b) The transverse Lyapunov exponents of the chaotic saddle and the period-3 attractor, Λ_T^S and Λ_T^O, respectively, versus the bifurcation parameter a in model equation (3).

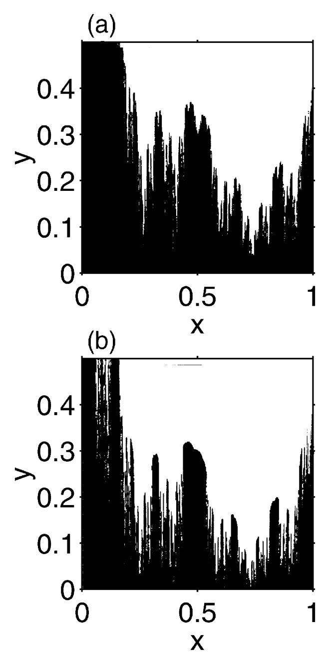

Fig. 3. The basins of the period-3 attractor (in black) and the attractor at infinity (in blank) for: (a) $a = 1.7$ ($\Lambda_T^S \approx -0.034$); (b) $a = 1.8$ ($\Lambda_T^S \approx 0.023$).

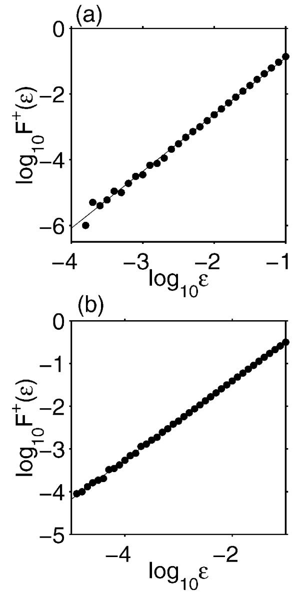

Fig. 4. $F^+(\epsilon)$ versus ϵ on a logarithmic scale for: (a) $a = 1.7$; (b) $a = 1.8$.

with similar transverse Lyapunov exponent, say, $\Lambda_T^S \approx -0.034$. In that case, the scaling exponent is proportional to $|\Lambda_T^S|$ which is close to zero [3,7]. The largeness of the scaling exponent γ for $|\Lambda_T^S| \gtrsim 0$, regardless of whether Λ_T^S is positive or negative, is a general feature of pseudo-riddling, in contrast to riddled basins of chaotic attractors. Physically, such a large exponent means that it is significantly more difficult for trajectories with random initial conditions near the invariant subspace to asymptote to the attractor off the invariant subspace. The dynamical reason lies in the finite lifetime τ_O of the chaotic saddle: a trajectory will approach the periodic attractor in a time given by τ_O. When $|\Lambda_T^S| \gtrsim 0$, it usually takes a long time for trajectories to escape the finite-time transverse attraction of the chaotic saddle in order to asymptote to the attractor off the invariant subspace.

4. An analytic example and scaling laws

To better understand the phenomenon of pseudo-riddling and the possible universal scaling behavior associated with it, we construct a simple analyzable model that captures the main qualitative features required for pseudo-riddling. We focus on the physically interesting case where a large number of unstable periodic orbits embedded in the chaotic saddle is transversely unstable so that the saddle itself is marginally transversely stable (or unstable). The model is the following two-dimensional map defined for $-\infty < x < \infty$ and $0 \le y < \infty$:

$$x_{n+1} = \begin{cases} h(x_n), & x_n < 0, \\ \dfrac{1+q}{p} x_n, & 0 < x_n < p, \\ \dfrac{1+q}{1-p}(1-x_n), & x_n > p, \end{cases} \qquad y_{n+1} = \begin{cases} e^{-\Gamma} y_n, & x_n < 0 \text{ and } 0 \le y_n < 1, \\ c y_n, & 0 < x_n < p < \frac{1}{2} \text{ and } 0 \le y_n < 1, \\ d y_n, & x_n > p \text{ and } 0 \le y_n < 1, \end{cases} \tag{5}$$

where $q \gtrsim 0$, $0 < p < 1$, $c > 1$, $0 < d < 1$, and $\Gamma > 0$. The map $h(x)$ is chosen such that it has a stable fixed-point **O** in $x < 0$, as shown in Fig. 5. Since $q \gtrsim 0$, we see that the x-dynamics has a chaotic saddle in (0, 1)

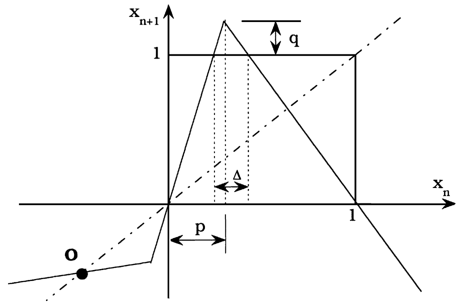

Fig. 5. The x-dynamics in the analyzable model equation (5).

with the following average lifetime:

$$\tau_{\mathrm{O}} = [\ln(1-\Delta)^{-1}]^{-1} = \frac{1}{\ln(1+q)} \approx \frac{1}{q}, \tag{6}$$

and almost all initial conditions eventually asymptote to the fixed-point attractor **O**, which is the dynamics in the invariant subspace $y = 0$. The y-dynamics is described by a simple expansion–contraction process for $0 \leq y < 1$, and we assume there is another attractor **A** located at $y > 1$ and any trajectory with $y > 1$ asymptotes to it rapidly. The transverse Lyapunov exponents of the fixed-point attractor and the chaotic saddle are

$$\Lambda_{\mathrm{T}}^{\mathrm{O}} = -\Gamma < 0, \qquad \Lambda_{\mathrm{T}}^{\mathrm{S}} = \left(\frac{p}{q}\right) \ln c + \left[\frac{1-p}{q}\right] \ln d, \tag{7}$$

respectively. Choosing p as the bifurcation parameter, we see that $\Lambda_{\mathrm{T}}^{\mathrm{S}}$ crosses zero from the negative side when p passes through the critical point $p_{\mathrm{c}} = |\ln d|/(\ln c + |\ln d|)$. Letting $Y = -\ln y$, we obtain the following dynamics in Y:

$$Y_{n+1} = \alpha_n + Y_n, \tag{8}$$

where $\alpha_n = -\ln c < 0$ if $0 < x_n < p$ and $\alpha_n = -\ln d > 0$ if $p < x_n < 1$. Since the x-dynamics is chaotic for $0 < x < 1$ in time τ_{O}, we see that the dynamics in Y_n is a *finite-time random walk*. It is finite-time because the chaotic saddle in $y = 0$ has a finite lifetime τ_{O}. A trajectory in one of the tongues located at some transversely unstable periodic orbits embedded in the chaotic saddle behaves, in the phase space, like a random walker before it is attracted to either the periodic attractor **O** in $y = 0$ or to the other attractor **A**. Focusing on the situation where $p \approx p_{\mathrm{c}}$ so that $\Lambda_{\mathrm{T}}^{\mathrm{S}} \approx 0$, the random walk dynamics can be described by the following drift–diffusion equation in time τ_{O} [26] [1]:

$$\frac{\partial P}{\partial t} + \nu \frac{\partial P}{\partial Y} = D \frac{\partial^2 P}{\partial Y^2}, \tag{9}$$

where $P(Y, t)$ stands for the probability distribution for Y, $\nu = -\Lambda_{\mathrm{T}}^{\mathrm{S}} \approx 0$ is the average drift and $D = \frac{1}{2}\langle(\delta Y - \langle \delta Y \rangle)^2\rangle$ is the diffusion coefficient. Choosing initial conditions from a line at $Y_0 = 1/\ln \epsilon$ $(y = \epsilon)$, we have the following initial condition for the diffusion equation:

$$P(Y, 0) = \delta(Y - Y_0). \tag{10}$$

[1] After submitting this paper, we became aware of the work of Dronov and Ott [38], which contains a more accurate derivation of the scaling laws.

Since trajectories having $y > 1$ are lost to the attractor **A** at $y = 1$, we have an absorbing boundary at $Y = 0$ $(y = 1)$:

$$P(0,t) = 0, \quad t < \tau_O. \tag{11}$$

To solve Eq. (9) with the initial condition equation (10) and the boundary condition equation (11), we make use of the standard Laplace-transform technique [27]. Letting $\bar{P}(Y,s)$ be the Laplace transform of $P(Y,t)$:

$$\bar{P}(Y,s) = \int_0^\infty e^{-st} P(Y,t)\,dt, \tag{12}$$

we obtain the following equation for $\bar{P}(Y,s)$:

$$D\frac{\partial^2 \bar{P}}{\partial Y^2} - \nu\frac{\partial \bar{P}}{\partial Y} - s\bar{P} = -\delta(Y - Y_0) \tag{13}$$

with the boundary condition

$$\bar{P}(0,s) = \bar{P}(\infty,s) = 0. \tag{14}$$

The solution to Eqs. (13) and (14) is

$$\begin{aligned} \bar{P}(Y,s) &= \frac{1}{D(P_+ - P_-)}[-e^{P_- Y_0 - P_+ Y} + \Theta(Y_0 - Y)\, e^{P_-(Y_0 - Y)} + \Theta(Y - Y_0)\, e^{-P_+(Y - Y_0)}], \\ P_\pm &= \frac{-\nu + \sqrt{\nu^2 + 4sD}}{2D}, \end{aligned} \tag{15}$$

where $\Theta(x)$ is the Heaviside step function. Since $\int_0^\infty P(Y,t)\,dY$ is the probability that the walker is still undergoing diffusion at time t, the probability for a trajectory to asymptote to the attractor **A** in time τ_O is

$$F^+(\epsilon) = 1 - \int_0^\infty P(Y,\tau_O)\,dY. \tag{16}$$

As a crude approximation, we assume that walkers who are still diffusing for time $t > \tau_O$ asymptote to the fixed-point attractor **O**. We thus obtain

$$F^+(\epsilon) = 1 - \frac{1}{2\pi i}\int_{\sigma - i\infty}^{\sigma + i\infty} ds\, e^{s\tau_O}\int_0^\infty dY\, \bar{P}(Y,s) = \frac{1}{2\pi i}\int_\infty^\infty \frac{d\omega}{\omega}\, e^{i\omega\tau_O}\exp\left[\frac{\ln\epsilon}{\sqrt{D}}\sqrt{i\omega + \frac{\nu^2}{4D}}\right]. \tag{17}$$

In the case, where $\tau_O \to \infty$, a closed expression for $F^+(\epsilon)$ can be obtained. Note that in this case, the significant contribution to the integral in Eq. (17) is the small ω range. Expanding the exponent in the integral in Eq. (17):

$$\frac{\ln\epsilon}{\sqrt{D}}\sqrt{i\omega + \frac{\nu^2}{4D}} \approx \frac{\nu\ln(1/\epsilon)}{2D} + i\frac{\ln(1/\epsilon)\omega}{\nu} + \frac{\ln(1/\epsilon)D\omega^2}{\nu^3} + \cdots,$$

we obtain

$$F^+(\epsilon) \approx \frac{1}{2}\exp\left(-\frac{\nu\ln(1/\epsilon)}{2D}\right)\operatorname{erf}\left(\frac{\tau_O}{2}\sqrt{\frac{\nu^3}{\ln(1/\epsilon)}D}\right),$$

where $\operatorname{erf}(z)$ is the error function. Using $\operatorname{erf}(z) \approx 1 - (1/\sqrt{\pi})(1/z)\,e^{-z^2}$, we obtain

$$F^+(\epsilon) \sim \epsilon^{\nu/D}\left[\frac{1}{2} - \frac{1}{\tau_O\sqrt{\pi}}\sqrt{\frac{D}{\nu^3}|\ln\epsilon|}\exp\left(-\frac{\tau_O^2\nu^3}{4D|\ln\epsilon|}\right)\right]. \tag{18}$$

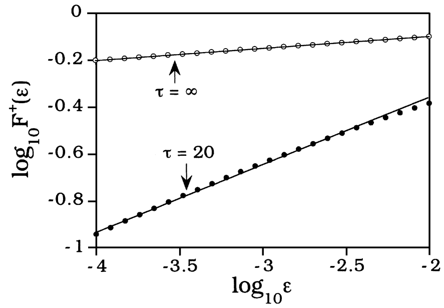

Fig. 6. Theoretically predicted scaling relations between $F^{+}(\epsilon)$ and ϵ for different values of lifetime of the chaotic saddle in the invariant subspace.

Fig. 6 shows $\log_{10} F^{+}(\epsilon)$ versus $\log_{10} \epsilon$, where the integration in Eq. (17) is done numerically and the parameters are chosen to mimic the parameter setting in our numerical example (Eq. (3)): $\nu = 0.05$, $D = 1$, and $\tau_{\rm O} = 20$. We see that the algebraic scaling law (4) holds well, in agreement with Figs. 4(a) and (b). The dashed straight line in Fig. 6 denotes the case where $\tau_{\rm O} \to \infty$. We see that indeed, the decay behavior for finite $\tau_{\rm O}$ is generally faster than that for the case of a chaotic attractor ($\tau_{\rm O} = \infty$) in the invariant subspace, in agreement with our numerical experiments of Eq. (3). Note that Eq. (18), or more generally, Eq. (17), includes the case of a chaotic attractor ($\tau_{\rm O} = \infty$) as a special case where it was found previously that $F^{+}(\epsilon) \sim \epsilon^{\nu/D}$ [3].

5. Blowout bifurcation of non-attracting chaotic saddles

When the dynamical invariant set in the invariant subspace is a chaotic attractor, the bifurcation at which the attractor loses its transverse stability is called *blowout* bifurcation [5,28,29]. We notice from our numerical and analytic models that the transverse stability of the chaotic saddle in the invariant subspace changes smoothly from being stable to unstable as the bifurcation parameter changes. A natural question is: what is the dynamical character associated with the blowout bifurcation of the chaotic saddle? Here we argue that at the bifurcation, there is a sudden extension of the chaotic saddle into the entire phase space [24].

The basic argument goes as follows. Before the bifurcation, the chaotic saddle is restricted to the invariant subspace. After the bifurcation, the transverse instability of the chaotic saddle stipulates that it acquire infinitely more new pieces outside the invariant subspace, which were not existent before the bifurcation. To see why, recall that a chaotic saddle is globally non-attracting and it has a basin of attraction of vanishing volume in the phase space. Nonetheless, a *conditionally invariant measure* can still be defined on the saddle.[2] Consider a trajectory on the chaotic saddle in $\mathcal{M}$ with respect to the conditionally invariant measure: call it a *conditional* trajectory. By continuity, a trajectory in the vicinity of the invariant space is also a conditional trajectory. For $\Lambda_{\rm T}^{\rm S} < 0$, the conditionally invariant measure on the chaotic saddle is transverse stable. That is, the chaotic saddle tends to attract nearby conditional trajectories in the transverse directions. Thus, the chaotic saddle is confined within the invariant subspace and it is *isolated* from the remaining of the phase space. For $\Lambda_{\rm T}^{\rm S} > 0$, the conditionally invariant measure on the chaotic saddle becomes unstable. Now a conditional trajectory in the neighborhood of the chaotic saddle

[2] A conditionally invariant measure on a chaotic saddle can be defined as follows [30]. Imagine that we enclose the saddle by a cube C in the phase space and we sprinkle a very large number $N(0)$ of initial conditions uniformly in the cube. The number of trajectories that still remain in C is $N(t) \approx N(0)\,{\rm e}^{-t/\tau}$, where τ is the average lifetime of the chaotic saddle. Let $N_0(\eta, t, C)$ be the number of trajectories that are in C at time ηt, where $0 < \eta < 1$. The conditionally invariant measure is defined to be $\mu_0(C) = \lim_{t\to+\infty}\lim_{n(0)\to\infty} N_0(\eta, t, C)/N(t)$.

is typically repelled away from it asymptotically. Since the trajectory is conditional, it remains conditional under the dynamics even though it is no longer confined within the invariant subspace. The corresponding measure that supports the trajectory must be conditional and, hence, it defines a chaotic saddle that *extends* beyond the invariant subspace $\mathcal{M}$ in the transverse subspaces. As a consequence, a sudden enlargement, or a metamorphosis, of the chaotic saddle occurs as $\Lambda_{\mathrm{T}}^{\mathrm{S}}$ becomes positive. The newly acquired infinite pieces of the chaotic saddle do not exist before the bifurcation: they are created at the bifurcation when the chaotic saddle in the invariant subspace becomes transversely unstable. [3]

The extension of the chaotic saddle in the invariant subspace into the full phase space after the blowout bifurcation can also be understood by using the analyzable model equation (5). Consider a trajectory in the vicinity of the chaotic saddle in the invariant subspace. The y-variable of the trajectory obeys Eq. (8), the random walk model. Taking the time average of Eq. (8), we obtain $\bar{Y}_{n+1} = \bar{\alpha}_n + \bar{Y}_n$. Since α_n is a random variable which takes on the values $-\ln c$ and $-\ln d$ with probabilities p/q and $(1-p)/q$, respectively, we have

$$\bar{\alpha}_n = \frac{p}{q}(-\ln c) + \frac{1-p}{q}(-\ln d) = -\Lambda_{\mathrm{T}}^{\mathrm{S}}.$$

Immediately after the blowout bifurcation, we have $\Lambda_{\mathrm{T}}^{\mathrm{S}} \gtrsim 0$ and, hence, $\bar{Y}_{n+1} < \bar{Y}_n$, which indicates that $\bar{y}_{n+1} > \bar{y}_n$. Since: (1) the change in y_n is finite in one iteration, and (2) on an average y_n increases for small y_n, we conclude that y_n cannot reach zero asymptotically. Thus, the trajectory, which is initiated in an arbitrarily small transverse neighborhood of the chaotic saddle in the invariant subspace, can no longer be restricted to the invariant subspace and it must lie in the full phase space. Since the trajectory starts in the immediate vicinity of the chaotic saddle in the invariant subspace, it must still be in the vicinity of the new chaotic saddle after the bifurcation, which now extends into the full phase space.

The above scenario for the blowout bifurcation of the chaotic saddle can be observed easily in numerical models such as equation (3). To compute a long continuous trajectory on a chaotic saddle, we make use of the PIM-triple algorithm. [4] Figs. 7(a) and (b) show bifurcation diagrams of the chaotic saddle, where the dynamical variables x_n and y_n of PIM-triple trajectories on chaotic saddles are plotted versus the parameter a for $1.7 \leq a \leq 1.8$. Before the blowout bifurcation, the saddle is apparently confined in the invariant subspace $y = 0$. PIM-triple trajectories on the saddle start to burst out of $y = 0$ after the bifurcation, as shown in Fig. 7(b). The bursts seen for $a < a_{\mathrm{c}} \approx 1.75$ in Fig. 7(b) are transients. To better visualize the chaotic saddle, in Figs. 8(a) and (b), we show the PIM-triple trajectories (plotted in black), together with the basin (in gray) of the period-3 stable attractor (large filled circles on the x-axis) in the invariant subspace, for $a = 1.7 < a_{\mathrm{c}}$ (before blowout bifurcation) and $a = 1.8$ (after the bifurcation), respectively. Apparently, for $a = 1.7$, the saddle is confined in the invariant subspace $y = 0$, while for $a = 1.8$, the chaotic saddle spreads in the basin of the stable periodic attractor in $y = 0$, and the Lyapunov

[3] Bifurcations of chaotic saddles have been investigated before. For instance, two chaotic saddles can collide with each other as a system parameter changes through a critical value, resulting in physically observable phenomena such as basin boundary metamorphosis [31,32] and enhancement of chaotic scattering in open Hamiltonian systems [33,34]. More recently, a homoclinic bifurcation has been identified after which a chaotic saddle acquires new pieces that were located at a finite distance from the saddle and were not part of the chaotic saddle before the bifurcation [35]. All these bifurcations were investigated for low-dimensional chaotic systems in which chaotic sets have only one positive Lyapunov exponent. Blowout bifurcation of the chaotic saddle discussed in [24] and here is a high-dimensional phenomenon where the chaotic saddle after the bifurcation possesses more than one positive Lyapunov exponent.

[4] For two-dimensional hyperbolic maps, it can be proven that the PIM-triple algorithm in [25] yields numerical trajectories that can stay arbitrarily close to the chaotic saddle. For non-hyperbolic cases, if the map is invertible, numerical evidence suggests that the algorithm is still capable of yielding an approximate natural measure for the chaotic saddle [36]. Our model equation (3) is a two-dimensional non-invertible map, as most model systems utilized previously in the study of riddled basins. Thus, in our case, there is no assurance that the PIM-triple algorithm would generate an approximate trajectory on a chaotic saddle. Nonetheless, we find that the algorithm generally yields trajectories that are consistent with the dynamics (e.g. Figs. 8(a) and (b)).

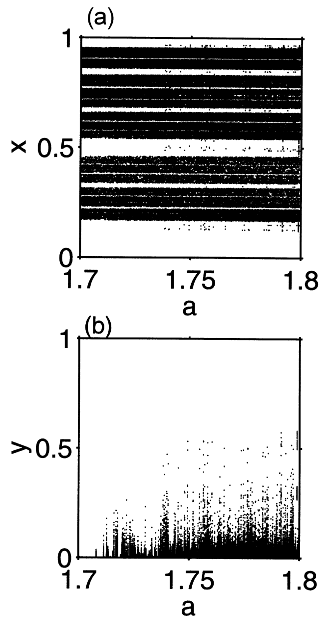

Fig. 7. For the numerical model equation (3), bifurcation diagram of the chaotic saddle near the blowout bifurcation at $a_c \approx 1.75$: (a) x versus a, and (b) y versus a, where x and y are the dynamical variables of a PIM-triple trajectory on the chaotic saddle. There is an extension of the saddle beyond the invariant subspace $y = 0$ at the bifurcation. The trajectory points with $y > 0$ seen before the bifurcation are transients. Asymptotically, there is a sudden extension of the chaotic saddle into the full phase space at the blowout bifurcation.

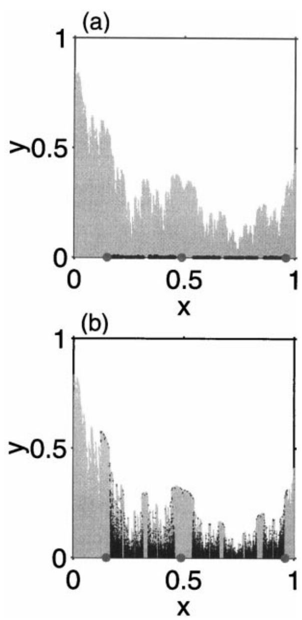

Fig. 8. PIM-triple trajectories (plotted in black), together with the basin (in gray) of the period-3 stable attractor (large filled circles on the x-axis) in the invariant subspace, for: (a) $a = 1.7 < a_c$ (before blowout bifurcation); (b) $a = 1.8$ (after the bifurcation).

exponents of the saddle are $\lambda_1 \approx 0.51$ and $\lambda_2 \approx 0.006$. In general, we find that $a > a_c$, the chaotic saddles are high-dimensional because they have two positive Lyapunov exponents.

6. Discussions

The phenomenon of riddling has been an active area of research in chaotic dynamics [1–8]. Although riddling relies on systems' possessing one or more invariant subspaces, the presence of invariant properties is common in models of dynamical systems. Symmetry, which usually leads to the existence of an invariant subspace, is perhaps not a rare property in dynamical systems. Riddling is relevant to spatio-temporal chaotic dynamics because spatially extended dynamical systems such as coupled oscillators often possess an invariant subspace: the synchronization manifold [4,9–11]. Riddling is also closely related to the phenomenon of on–off intermittency [5,16–23,28]. Most of the existing work on riddling, however, focused on the case where there is a chaotic attractor in the invariant subspace.

The main motivation of this paper comes from the fact that chaos can not only occur on chaotic attractors, but it can also come from non-attracting chaotic saddles [14]. In particular, a chaotic system can operate in one of the infinite number of periodic windows in which a chaotic saddle and a stable periodic attractor coexist. If the dynamics in the invariant subspace occurs in a periodic window, the question is whether riddling can still be expected. We have provided a firm answer to this question in the present work. Specifically, we show, with the support of analyses and numerical evidence, that due to the dynamical interplay between the non-attracting chaotic saddle and the stable periodic attractor, riddling can then be more pervasive than the case where there is a chaotic attractor in the invariant subspace. Our scaling analysis also generalizes results obtained in previous studies of riddling. Since periodic windows are dense and structurally stable and therefore are common in nonlinear systems, we expect our results to be relevant to problems such as synchronization of nonlinear oscillators [9–11,37].

Finally, we wish to suggest how the phenomenon reported in this paper can possibly be observed in experiments. Take, e.g. the experimental system consisting of a number of coupled chaotic electronic circuits by Heagy, Carroll, and Pecora to study riddled basins [4]. In the original experiment, the parameters of the chaotic circuits are chosen so that each circuit, when isolated, exhibits a chaotic attractor. In order to observe pseudo-riddling, one can simply adjust the parameters of each circuit so that it falls in a periodic window and examine the basin of the synchronous periodic attractor. As we have predicted in this paper, pseudo-riddling can occur regardless of the transverse stability of the chaotic saddle in the periodic window, which means that, in the experimental situation described, the range of the coupling conductance between the circuits for pseudo-riddling to be observed can be much larger than that for the case where each circuit exhibits a chaotic attractor. Specifically, let r be an internal parameter for each individual circuit, and let r_1 and r_2 be two parameter values for which the circuit exhibits a chaotic attractor and periodic window, respectively, where $r_1 \approx r_2$. Since r_1 is close to r_2, the transverse Lyapunov spectrum of the chaotic attractor at r_1 is close to that of the chaotic saddle at r_2. For each case, one can then change the coupling parameter systematically and measure the range of this parameter for which pseudo-riddling can be observed (say, visually). Our point is that it is easier to observe (pseudo-) riddling for $r = r_2$ because, for $r = r_1$, riddling disappears as soon as the chaotic attractor becomes transversely unstable, while for $r = r_2$, pseudo-riddling still exists even when the chaotic saddle becomes transversely unstable.

Acknowledgements

I thank Prof. Celso Grebogi for discussions and R. Buniy for assisting in obtaining the solution to the diffusion equation. This work was supported by AFOSR under Grant No. F49620-98-1-0400 and by NSF under Grant No. PHY-9722156.

References

[1] A. Pikovsky, P. Grassberger, J. Phys. A 24 (1991) 4587.
[2] J.C. Alexander, J.A. Yorke, Z. You, I. Kan, Int. J. Bifur. Chaos 2 (1992) 795.
[3] E. Ott, J.C. Alexander, I. Kan, J.C. Sommerer, J.A. Yorke, Physica D 76 (1994) 384.
[4] J.F. Heagy, T.L. Carroll, L.M. Pecora, Phys. Rev. Lett. 73 (1994) 3528.
[5] Y.-C. Lai, C. Grebogi, Phys. Rev. E 52 (1995) R3313.
[6] Y.-C. Lai, C. Grebogi, J.A. Yorke, S.C. Venkataramani, Phys. Rev. Lett. 77 (1996) 55.
[7] Y.-C. Lai, C. Grebogi, Phys. Rev. Lett. 77 (1996) 5047.
[8] T. Kapitaniak, Y. Maistrenko, A. Stefanski, J. Brindley, Phys. Rev. E 57 (1998) R6253.
[9] J.F. Heagy, T.L. Carroll, L.M. Pecora, Phys. Rev. E 50 (1994) 1874.
[10] J.F. Heagy, L.M. Pecora, T.L. Carroll, Phys. Rev. Lett. 74 (1995) 4185.
[11] L.M. Pecora, T.L. Carroll, Phys. Rev. Lett. 80 (1998) 2109.
[12] M.V. Jacobson, Commun. Math. Phys. 81 (1981) 39.
[13] J. Graczyk, G. Światek, Ann. Math. 146 (1996) 1.
[14] T.Y. Li, J.A. Yorke, Am. Math. Monthly 82 (1975) 985.
[15] Y.-C. Lai, C. Grebogi, Phys. Rev. Lett. 83 (1999) 2926.
[16] E.A. Spiegel, Ann. NY Acad. Sci. 617 (1981) 305.
[17] A.S. Pikovsky, Z. Phys. B 55 (1984) 149.
[18] H. Fujisaka, T. Yamada, Prog. Theoret. Phys. 74 (1985) 919
[19] H. Fujisaka, T. Yamada, Prog. Theoret. Phys. 75 (1986) 1087.
[20] A.S. Pikovsky, Phys. Lett. A 165 (1992) 33.
[21] N. Platt, E.A. Spiegel, C. Tresser, Phys. Rev. Lett. 70 (1993) 279.
[22] Y.-C. Lai, Phys. Rev. E 53 (1996) R4267.
[23] Y.-C. Lai, Phys. Rev. E 54 (1996) 321.
[24] T. Kapitaniak, Y.-C. Lai, C. Grebogi, Phys. Lett. A 259 (1999) 445.
[25] H.E. Nusse, J.A. Yorke, Physica D 36 (1989) 137.
[26] W. Feller, An Introduction to Probability Theory and its Applications, Wiley, New York, 1966.
[27] J. Mathews, R.L. Walker, Mathematical Methods of Physics, Addison-Wesley, Reading, MA, 1970.
[28] E. Ott, J.C. Sommerer, Phys. Lett. A 188 (1994) 39.
[29] Y. Nagai, Y.-C. Lai, Phys. Rev. E 56 (1997) 4031.
[30] G.H. Hsu, E. Ott, C. Grebogi, Phys. Lett. A 127 (1988) 199.
[31] C. Grebogi, E. Ott, J.A. Yorke, Phys. Rev. Lett. 56 (1986) 1011.
[32] C. Grebogi, E. Ott, J.A. Yorke, Physica D 24 (1987) 243.
[33] Y.-C. Lai, C. Grebogi, R. Blümel, I. Kan, Phys. Rev. Lett. 71 (1993) 2212.
[34] Y.-C. Lai, C. Grebogi, Phys. Rev. E 49 (1994) 3761.
[35] C. Robert, K.T. Alligood, E. Ott, J.A. Yorke, Phys. Rev. Lett. 80 (1998) 4867.
[36] J. Jacobs, E. Ott, C. Grebogi, Physica D 108 (1997) 1.
[37] L.M. Pecora, T.L. Carroll, Phys. Rev. Lett. 64 (1990) 821.
[38] V. Dronov, E. Ott, Chaos 10 (2000) 291.